

## Dendritic growth in a channel

David A. Kessler

*Department of Physics, University of Michigan, Ann Arbor, Michigan 48109*

Joel Koplik and Herbert Levine

*Schlumberger-Doll Research, Old Quarry Road, Ridgefield, Connecticut 06877-4108*

(Received 9 June 1986)

We study the growth of dendritic crystals from a supersaturated solution in a channel geometry. This model provides a continuous interpolation between the Saffman-Taylor problem and the (two-dimensional) free-space dendrite. We derive an integral equation for the shape of steady-state propagating fingers, which we treat by discretizing the curve and solving the resulting set of nonlinear algebraic equations by Newton's method. For general Peclet numbers, in the absence of anisotropy the finger widths are always greater than half the channel width, but with anisotropy all widths are obtained. The numerical results are in rough agreement with an approximate WKB treatment for small anisotropy and zero Peclet number. Finally, we speculate on the emergence of sidebranches in this system.

### I. INTRODUCTION

The past few years have seen considerable progress made in our understanding of interfacial pattern formation.<sup>1</sup> The paradigm of microscopic solvability has been successfully applied to local models,<sup>2,3</sup> two-dimensional flow in a Hele-Shaw cell<sup>4,5</sup> (the Saffman-Taylor finger), dendritic growth from a pure supercooled melt,<sup>6,7</sup> and directional solidification.<sup>8</sup> This method relies on the existence of a solvability condition whenever one attempts to find steady-state solutions of the evolution equations in the presence of finite surface tension. This condition chooses the allowed shape and growth rate and also has important implications for the subsequent stability analysis.

The purpose of this paper is to discuss a slightly different pattern forming system. We imagine a supersaturated solution placed in the narrow gap between two parallel plates, with impermeable top and sidewall boundaries. This device is just the classic Hele-Shaw cell used for multiphase flow, but we now consider nucleating a crystal and letting it grow down the channel. The crystal will then form a growing finger, possibly a dendritic pattern with sidebranches starting some distance away from the tip. It is this pattern that we wish to understand. Experiments on this type of system have been performed by Honjo, Ohta, and Sawada,<sup>9</sup> who however only studied the limiting case of nearly free dendrites.

The importance of this system is that, as we will show, its dynamics of this system can be used to interpolate between the Saffman-Taylor problem and the two-dimensional free dendrite. We define a dimensionless Peclet number  $p$  as the ratio of channel width to diffusion length; this parameter controls the importance of the finite time scale for solute diffusion. At low  $p$  (narrow channels), we will find that relaxation occurs sufficiently quickly that one may replace the diffusion Green's function by that for Laplace's equation. The interfacial evolution equations are then exactly those which apply to mul-

tiphase flow in Hele-Shaw cells, albeit with additional anisotropy arising from the crystal structure. The idea of anisotropy in the Saffman-Taylor problem has also arisen independently from experiments in Hele-Shaw cells with grooved plates.<sup>10</sup>

As the channel widens, the tip is less severely affected by the boundary conditions on the side walls. In the limit of high  $p$  (large width), the pattern is described by the free dendrite equations with corrections that only become important far from the tip. The known results for two-dimensional free dendritic growth should then be recovered smoothly at large  $p$ .

This type of interpolation is useful in attempting to understand some of the remaining mysteries of interfacial patterns. For example, it is by now well established that the two-dimensional Saffman-Taylor<sup>11</sup> equation predicts an asymptotic width of  $\frac{1}{2}$  as we approach zero surface tension.<sup>12-14</sup> It is important to understand how this limit arises, and how it changes upon the addition of complicating terms in the evolution equation arising either from anisotropy or finite diffusion constant. The importance of the latter is emphasized by experimental results<sup>15,16</sup> clearly indicating widths below  $\frac{1}{2}$ . We will argue and then demonstrate numerically that, in the isotropic case, there is a lower bound on  $\lambda$  which is a function of  $p$ . We expect that  $\lambda$  increases from  $\frac{1}{2}$  to 1 as  $p$  goes from zero to infinity. We will also show that the presence of even infinitesimal anisotropy completely alters this picture. Instead, the presence of finite anisotropy allows us to construct steady-state solutions at all  $\lambda$  and  $p$ , provided we choose the surface tension to satisfy the solvability condition.

Perhaps an even more important puzzle is the nature of sidebranching. In the Saffman-Taylor problem, there appears to be a nonlinear instability which gives rise to either "thumbing" (antisymmetric mode) or "tip-splitting" (symmetric mode) at small enough surface tension.<sup>15-19</sup> Experimentally, adding anisotropy converts these modes into repeated sidebranching.<sup>10</sup> This suggests that sidebranching in free dendritic growth may also arise as a

noise-induced finite amplitude effect around a linearly stable needle crystal.<sup>20</sup> Our model can be used to investigate this possibility by varying the channel size. We will present a simple picture of this finite amplitude instability which supports the above picture, but a final resolution awaits additional study.

The outline of this paper is as follows. In Sec. II, we define our model and derive an integral equation governing the pattern evolution. In Sec. III, we derive the asymptotic shape required of steady-state solutions and then describe our numerical approach to find the selected steady-state shape. In Sec. IV (and in the Appendix), we focus on the results for a zero Peclet number, in particular, the effects of anisotropy in determining the pattern and its growth rate. We analytically derive the scaling of  $\lambda$  versus  $\gamma$  at fixed  $\epsilon$  and qualitatively verify the result numerically. Results at finite  $p$  will be presented and discussed in Sec. V. Finally, in Sec. VI, we discuss our simplified explanation of the nonlinear instability found originally in the pure Saffman-Taylor problem and speculate on how this idea can be used to understand sidebranching.

## II. GROWTH IN A CHANNEL

This paper is concerned with growth processes taking place in a particular confined geometry—a narrow gap, finite-width channel between two inert plates. We consider a supersaturated solution in the channel with growth nucleated at one end. We assume that the growth is two dimensional and diffusion limited, with the rate controlled by the arrival of solute at the growing crystal. The solute concentration satisfies the diffusion equation

$$D\nabla^2 c = \frac{\partial c}{\partial t}, \quad (1)$$

with the boundary condition  $c(x, y \rightarrow \infty) = c_\infty$ , where  $c_\infty$  is greater than  $c_{eq}$ , the solute concentration in liquid in equilibrium with pure crystal. Because the side walls are impermeable, we have  $\partial c / \partial x |_{x=\pm a} = 0$ . The geometry of the channel is depicted in Fig. 1. We can define a dimensionless supersaturation by  $\tilde{\Delta} = (c_\infty - c_{eq}) / \Delta c_0$ , where  $\Delta c_0 = 1 - c_{eq}$  is the miscibility gap.

In addition, we have two boundary conditions at the moving interface. First, conservation of matter requires that

$$v_n \Delta c = D \left. \frac{\partial c}{\partial n} \right|_{\text{liquid}}, \quad (2)$$

where  $v_n$  is the normal velocity and  $\Delta c$  is the actual difference between solute concentration and crystal concentration ( $c=1$  for pure crystal) at the interface. As is well known, this gap is corrected from the planar interface result by surface tension:<sup>21</sup>

$$\Delta c = \Delta c_0 [1 - d_0(\theta)\kappa], \quad (3)$$

where  $d_0$  is the chemical capillary length. Often we will take  $d_0(\theta)$  to be anisotropic, with angular dependence  $\bar{d}_0(1 - \epsilon \cos\theta)$ , where  $\tan\theta = \partial y / \partial x$ . Finally, the assumption of local equilibrium ensures that the solute concentration at the interface satisfies

$$c_{\text{liquid}}(\mathbf{x}(s)) = 1 - \Delta c. \quad (4)$$

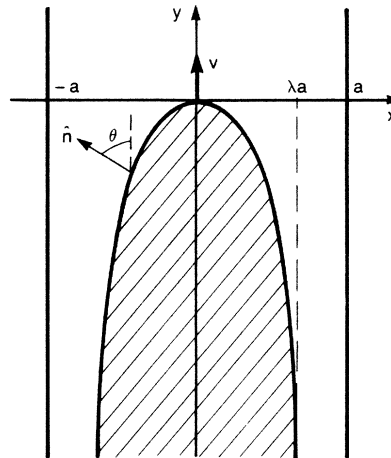


FIG. 1. Geometry of finger growth in a channel.

Equations (1)–(4) constitute the equations of motion for the interface.

We now specialize to the case of steady-state motion at velocity  $\mathbf{v} = v\hat{y}$ . If we introduce  $p = va/2D$  and measure lengths in units of  $a$ , then  $u \equiv (c_\infty - c) / \Delta c_0$  satisfies

$$\begin{aligned} \nabla^2 u + 2p \frac{\partial u}{\partial y} &= 0, \\ u(\mathbf{x}(s)) &= \tilde{\Delta} - \tilde{d}_0(\theta)\kappa, \\ -\hat{\mathbf{n}} \cdot \nabla u &= 2p\hat{\mathbf{n}}_y [1 - \tilde{d}_0(\theta)\kappa], \end{aligned} \quad (5)$$

with  $\tilde{d}_0 = d_0/a$ , and the field is evaluated on the liquid side of the interface. The above evolution equation can be put in the form of an integral equation for the interface. Let us define a continuation of the  $u$  field into the solid which we arbitrarily take to equal  $\tilde{\Delta}$ . Then, we can write down the most general solution of the diffusion equation as

$$\begin{aligned} u(x, y) &= \int \hat{\mathbf{n}}' \cdot \nabla' G(x, y; x(s'), y(s')) \phi_1(s') ds' \\ &\quad - \int G(x, y; x(s'), y(s')) \phi_2(s') ds', \end{aligned}$$

where the diffusive Green's function  $G(\mathbf{x}; \mathbf{x}')$  obeys

$$\nabla^2 G + 2p \frac{\partial G}{\partial y} = -\delta(x - x')\delta(y - y'),$$

$\partial G / \partial x |_{x=\pm 1} = 0$ , and  $G \rightarrow 0$  for  $y \rightarrow +\infty$ . This formula defines a charge layer  $\phi_1$  and a double layer  $\phi_2$ . To find these functions, we use the fact that the integral representation implies that the discontinuities across the interface are

$$[u(x, y)]_{\text{liquid-solid}} = \phi_1$$

and

$$[\hat{\mathbf{n}} \cdot \nabla u(x, y)]_{\text{liquid-solid}} = \phi_2 - 2p\hat{\mathbf{n}}_y \phi_1,$$

which can easily be verified by using the above definitions. Comparing this to Eq. (5), we derive  $\phi_1 = -\tilde{d}_0\kappa$  and  $\phi_2 = -2p\partial x / \partial s$ . Finally, if we evaluate the integrals for  $u$  slightly inside the crystal, we find the steady-state equation

$$\bar{\Delta} = - \int ds' (\hat{n} \cdot \nabla G) \bar{d}_0(\theta) \kappa + 2p \int G dx'. \quad (6)$$

We now need an explicit expression for the Green's function. The free-space version is

$$\int \frac{d^2k}{(2\pi)^2} \frac{e^{ik_x x} e^{ik_y y}}{k_x^2 + k_y^2 - 2ipk_y}.$$

By the method of images, the Green's function which sat-

$$G(x, y; x', y') = \frac{1}{4p} (e^{-p(y-y')} - p|y-y'|}) + \frac{1}{2} \sum_{n>0} \exp \left[ \frac{-p(y-y') - [(n\pi)^2 + p^2]^{1/2} |y-y'|}{[(n\pi)^2 + p^2]^{1/2} \cos[n\pi(x-x')]} \right], \quad (7)$$

As  $p \rightarrow 0$ , this Green's function approaches the result for Laplace's equation in the same geometry. In Sec. III, we will describe our method of numerically evaluating this function.

For large  $p$ , it is preferable to sum over  $n$  after performing the  $k$  integrals. This yields

$$G(x, y; x', y') = \frac{1}{\pi} e^{p(y'-y)} \sum_n K_0 \{ p[(x-x'+2n)^2 + (y-y')^2]^{1/2} \}. \quad (8)$$

As  $p$  goes to infinity, we redefine lengths by  $\tilde{x} = x/p$ ,  $\tilde{y} = y/p$ , and using the decay of  $K_0$  at large arguments, recover the free-space Green's function (the  $n=0$  term) with lengths measured in units of  $2D/v$ .

Finally, we need to consider the boundary conditions on the interface. Note that  $G$  approaches a constant for  $(y-y') \rightarrow -\infty$ . Imagine evaluating Eq. (6) for a point far down the interface. The constant in  $G$  must be chosen so that

$$\bar{\Delta} = 2p \int dx' \lim_{y \rightarrow \infty} G(x, y, x', y') \sim \frac{1}{2} \int dx'.$$

If the interface runs from  $x = -\lambda$  to  $x = +\lambda$ , we therefore derive  $\bar{\Delta} = \lambda$ . This can also be seen to be an immediate consequence of solute conservation in steady-state motion. For convenience, we can shift the Green's function by exactly  $(4p)^{-1}$  to cancel  $\bar{\Delta}$  on the left-hand side of the integral equation. With this convention, the Green's function falls to zero exponentially as  $y' \rightarrow -\infty$ .

### III. ASYMPTOTIC BEHAVIOR AND NUMERICAL METHOD

The steady-state shape we wish to solve for can be described by a symmetric function  $y(x)$  which approaches negative infinity as  $x \rightarrow \pm\lambda$ . We now derive the asymptotic behavior of this solution; this asymptotic behavior is crucial in implementing a numerical algorithm for determining the shape and selected velocity.

Consider solving for the field  $u$  in the gap between the interface and the channel side wall. Since we expect exponential convergence of  $x$  to  $\lambda$  as  $y \rightarrow -\infty$ , we assume

$$u - \bar{\Delta} \sim \cos[\alpha(1-x)] e^{\alpha y}, \quad (9a)$$

ifies the side-wall condition for symmetric fingers is therefore

$$\int \frac{d^2k}{(2\pi)^2} \sum_{n=-\infty}^{\infty} \frac{e^{ik_x(x+2n)} e^{ik_y y}}{k_x^2 + k_y^2 - 2ipk_y}.$$

For small Peclet numbers, it is convenient to do the sum over  $n$  first and then perform the integrals over  $k_y$  and  $k_x$ . We find

where the cosine ensures  $\partial u / \partial x|_{x=\pm\lambda} = 0$  and the differential equation requires  $\alpha'^2 + 2p\alpha' = \alpha^2$ . Now asymptotically we expect  $x(y) = \lambda - a_1 e^{\alpha y}$ , and therefore  $\kappa = a_1 \alpha'^2 e^{\alpha y}$ . The interfacial conditions to this order then require

$$\cos[\alpha(1-\lambda)] = -\alpha'^2 \bar{d}_0(1-\epsilon) a_1,$$

$$\alpha \sin[\alpha(1-\lambda)] = -2\alpha' p a_1.$$

Dividing, we find the rate of approach via the equation

$$\cot[\alpha(1-\lambda)] = \alpha \alpha' \bar{d}_0(1-\epsilon) / 2p. \quad (9b)$$

Note that (9a) and (9b) fix  $\alpha$  and  $\alpha'$ . We now carry the above computation to one higher order. We write

$$x(y) = \lambda - a_1 e^{\alpha y} - a_2 e^{2\alpha y},$$

$$u - \bar{\Delta} = \cos[\alpha(1-x)] e^{\alpha y} + b \cos[2\alpha(1-x)] e^{2\alpha y}.$$

Keeping all terms of the form  $e^{2\alpha y}$ , leads to the equations

$$b \cos[2\alpha(1-\lambda)] - a_1 \sin[\alpha(1-\lambda)] = -4a_2 \alpha'^2 \bar{d}_0(1-\epsilon),$$

$$2ab \sin[2\alpha(1-\lambda)] + 2a_1(\alpha^2 + \alpha'^2) \cos[\alpha(1-\lambda)] = -4a_2 \alpha' p + 2\bar{d}_0(1-\epsilon) p \alpha'^3 a_1^2,$$

which can be solved to yield

$$a_2/a_1^2 = \frac{2\alpha p + \bar{d}_0(1-\epsilon) \alpha'^3 \cot[2\alpha(1-\lambda)]}{2p \cot[2\alpha(1-\lambda)] - 4\bar{d}_0(1-\epsilon) \alpha \alpha'}. \quad (9c)$$

Again motivated by the Saffman-Taylor limit, we parametrize the interface as

$$y(x) = y_0(x) + z(x), \quad y_0(x) = \frac{1}{\alpha'} \ln \cos \left[ \frac{\pi x}{2\lambda} \right] \quad (10)$$

and discretize the interval  $0 \leq x \leq \lambda$  into  $N+1$  points. Furthermore, the curve is assumed symmetric around  $x=0$ . The boundary conditions derived above fix  $z(N)=0$  and  $\partial z / \partial x(N) = -a_2 / (a_1^2 \alpha')$ . The remaining  $N-1$  variables are determined by solving  $N-1$  nonlinear equations obtained by evaluating the integrals at the observation points  $x_i$ ,  $i=1, \dots, N-1$ . All integrals are done to  $O(1/N^2)$  and the resulting shape converges quadratically to the true shape. The actual solution of the equations is done by Newton's method using the IMSL (Ref. 22) solver ZSPOW, starting from an initial guess  $z_i=0$ .

In order to perform the above computation, we require computable expressions for the Green's function. At high Peclet number, a truncation of the series in Eq. (8) is sufficient. This is because convergence is uniform in  $x - x'$

in this limit. For  $p$  small, however, arbitrarily high values in  $n$  contribute for  $x \sim x'$  and a simple truncation is not valid. Instead, we add and subtract the sum in (7) evaluated at  $p = 0$  to write

$$\begin{aligned} & \frac{1}{2} \sum_n \frac{\exp\{-p(y-y') - [(n\pi)^2 + p^2]^{1/2} |y-y'|\}}{[(n\pi)^2 + p^2]^{1/2}} \cos[n\pi(x-x')] \\ &= -\frac{e^{-p(y-y')}}{4\pi} \ln[1 + e^{-2\pi|y-y'|} - 2e^{-\pi|y-y'|} \cos(\pi|x-x'|)] \\ &+ \frac{1}{2} \sum_n \left[ \frac{\exp\{-[(n\pi)^2 + p^2]^{1/2} |y-y'|\}}{[(n\pi)^2 + p^2]^{1/2}} - \frac{e^{-n\pi|y-y'|}}{n\pi} \right] e^{-p(y-y')} \cos[n\pi(x-x')]. \end{aligned}$$

The remaining summation now converges sufficiently rapidly to ensure that we can truncate the series to obtain a good approximation to  $G$ . When we take derivatives of  $G$ , we pick up additional problems with series convergence; again, these can be handled by further subtractions.

The program can be tested by a variety of means. First, the high and low Peclet versions of the Green's functions must match for intermediate values. Also, at small  $p$ , this problem goes over to the Saffman-Taylor problem (see the next section). This leads to constraints such as

$$\int_{-\lambda}^{\lambda} G(p=0) = 0, \quad \text{for } z(x) = 0,$$

inasmuch as  $y_0$  is the exact solution of the zero surface tension Saffman-Taylor problem. One can explicitly verify the fact that the discrete approximation to the integral converges as  $1/N^2$ ; any mistake in the discretization, such as incorrect handling of the singularity at  $x \sim x'$ , or incorrect treatment of the  $\delta$ -function singularity in curvature arising from the cusp at the tip, is immediately detectable.

The output of this program for fixed  $p$ ,  $\lambda$ , and  $d_0$  is a curve which in general has a discontinuity in its first derivative at the tip. This defines a mismatch function

$$f(\lambda, p, d_0) \equiv \frac{\partial z}{\partial x}(x=0) = \frac{-z_2 + 4z_1 - 3z_0}{2dx}, \quad (11)$$

where  $dx = 1/N$  is the spacing of the interpolation points in  $x$ . The allowed physical solutions have zero mismatch. Therefore, we can use  $f=0$  to solve parametrically for  $p$  as a function of  $\lambda$  and  $d_0$ . Since the length scale  $a$  is explicitly known, this immediately determines the selected velocity.

#### IV. THE SAFFMAN-TAYLOR LIMIT

As we have already mentioned, as the diffusion length becomes small compared to the channel width, the problem of dendritic growth becomes similar to the fluid mechanical problem studied by Saffman and Taylor. In crystals, the surface tension is in general anisotropic, in contrast to the purely isotropic equations valid in the flow case. The purpose of this section is to compute the effect that anisotropy has on the pattern selection.

Formally, we obtain the  $p=0$  limit by the rescaling

$$-\tilde{\Delta} + u = 2p\lambda\tilde{u}, \quad \tilde{d}_0 = 2p\lambda\gamma. \quad (12)$$

If we let  $p \rightarrow 0$ , the equations for the rescaled variables become

$$\begin{aligned} \nabla^2 \tilde{u} &= 0, \\ \tilde{u}_{\text{int}} &= -\gamma\kappa[1 - \epsilon \cos(m\theta)], \\ -\hat{\mathbf{n}} \cdot \nabla \tilde{u} |_{\text{int}} &= \hat{\mathbf{n}}_y / \lambda, \end{aligned} \quad (13)$$

with the boundary condition  $\tilde{u} \sim -y$  as  $y \rightarrow \infty$ . This is just an anisotropic version of the Saffman-Taylor problem with  $\gamma$  the usual inverse capillary number. Similarly, one can explicitly take the limit in (9a) of the rate of approach to  $x = \pm\lambda$  and find that  $\alpha' = \alpha$  satisfies

$$\cot\alpha(1-\lambda) = \lambda\gamma\alpha^2(1-\epsilon).$$

Aside from the anisotropy, this equation is the result derived previously by McLean and Saffman.<sup>23</sup>

It is by now well established for Hele-Shaw flow that the selected values of  $\lambda$ ,  $\lambda_i(\gamma)$ , approach  $\frac{1}{2}$  from above as  $\gamma$  goes to zero. The only stable solution is the narrowest member of this set, which we will denote  $\lambda^*$ . In crystal growth, the supersaturation  $\lambda$  is the experimental control parameter and  $\gamma$ , which contains the velocity, is the quantity we would like to predict. If the anisotropy were zero, no  $\lambda < \frac{1}{2}$  would permit steady-state motion. We can refer to the range  $0 \leq \lambda \leq \frac{1}{2}$  as the forbidden region.

We would now like to investigate the effect of finite anisotropy. We have computed the selected shape as a function of  $\lambda$  and  $\gamma$  by solving the limiting form of (6) and requiring zero mismatch. In Fig. 2, we have plotted the outcome of a typical set of calculations, for  $\epsilon = 0.10$  and fourfold asymmetry. As  $\gamma \rightarrow 0$ ,  $\lambda^*$  does not asymptote to  $\frac{1}{2}$  but instead continues well past this line. Our data suggest, in fact, that the forbidden region has completely disappeared! That is, at any finite anisotropy, all values of  $\lambda$  are accessible as we vary  $\gamma$ . Or, stated more conveniently for experimental test, steady-state motion is possible for all  $\lambda$ , with the selected value  $\gamma^*(\epsilon)$  having the power-law behavior  $\gamma^* \sim \epsilon^\sigma$ . We have verified this picture for several values of  $\epsilon$  and determined that  $\sigma$  is approximately  $1.5 \pm 0.4$ .

Recently, a WKB approach to the Saffman-Taylor problem<sup>12-14</sup> has succeeded in deriving the scaling

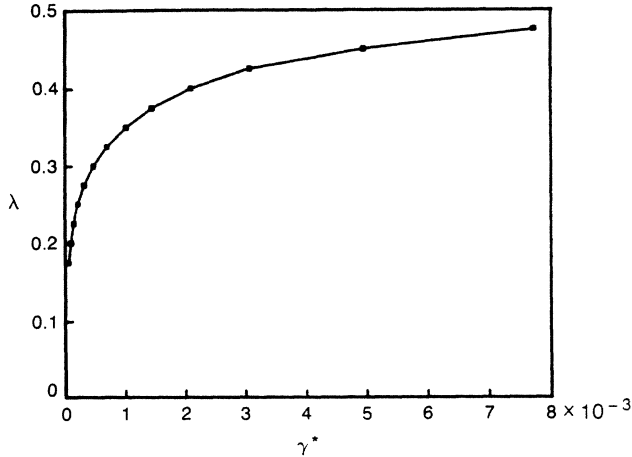


FIG. 2. Dependence of selected  $\gamma^*$  on channel width in the Saffman-Taylor limit, at  $\epsilon=0.1$ .

behavior  $(\lambda - \frac{1}{2}) \sim \gamma^{2/3}$ . In the Appendix, we generalize this treatment to the case of finite anisotropy. We find that for all  $\epsilon > 0$  and for all values of the symmetry index  $m$ , steady-state solutions exist at arbitrary width. The scaling laws derived for  $m=4$ , that  $\lambda \sim \gamma^{1/4}$  at fixed  $\epsilon$ , or  $\gamma \sim \epsilon^{7/4}$  at fixed  $\lambda$ , agree qualitatively with the numerical data presented here.

We would now like to connect this behavior to the known results for free dendritic growth. In that case there is convincing numerical evidence that, in the absence of anisotropy, steady-state solutions do not exist for any value of undercooling  $\Delta$ . In the language used here, the forbidden region is  $0 \leq \Delta \leq 1$ . Adding finite  $\epsilon$  allows solutions at all  $\Delta$ , with a power-law scaling of the same form as that described above. Now, free dendritic growth is just the  $p \rightarrow \infty$  limit of capillary tube growth where  $\Delta$  maps directly onto  $\lambda$ . Therefore, the obvious conjecture is that as  $p$  is decreased the forbidden region shrinks to  $\lambda < \frac{1}{2}$ , and that the role of anisotropy remains similar at all  $p$ .

## V. SOLUTIONS AT NONZERO PECELET NUMBER

We have carried out the same velocity selection calculations at finite Peclet number, with the results shown in Table I. The parameter values used were  $p=0.1$  and  $0.5$  and  $\epsilon=0, 0.05$  and  $0.1$ . The solution method is to fix  $p, \lambda$ , and  $\epsilon$  and then vary  $\gamma$  until no cusp is present at the tip. In effect, this fixes the capillary length  $\bar{d}_0$ , although one may turn the results around to obtain a prediction for the dendrite velocity as a function of the system parameters.

The principal qualitative result is that dendrite widths below  $\frac{1}{2}$  are never found in the absence of anisotropy, and in fact the smallest widths observed at  $\epsilon=0$  are always a finite amount above  $0.5$ . Furthermore, as  $p$  increases, the minimum  $\lambda$  for which solutions are found also increases. The numerical method has convergence problems due to noise when  $\gamma$  becomes too small (significantly below  $10^{-4}$ ), essentially for the same reasons as in the Saffman-Taylor problem. As a result, we have not been able to

TABLE I. Selected values of  $\gamma$  at various  $\epsilon$  and  $\lambda$  for  $p=0.1$  and  $0.5$ . An asterisk means no solution was found.

$\lambda$	$\epsilon=0$	$\epsilon=0.05$	$\epsilon=0.1$
	$p=0.1$		
0.2	*	$1.32 \times 10^{-4}$	$7.84 \times 10^{-5}$
0.4	*	$6.85 \times 10^{-4}$	$1.26 \times 10^{-3}$
0.5	*	$4.44 \times 10^{-3}$	$8.23 \times 10^{-3}$
0.55	$5.94 \times 10^{-3}$	$1.57 \times 10^{-2}$	$3.45 \times 10^{-2}$
0.6	$5.13 \times 10^{-3}$ $3.59 \times 10^{-2}$	$5.16 \times 10^{-3}$ $4.01 \times 10^{-2}$	$1.06 \times 10^{-3}$ $5.42 \times 10^{-2}$ $4.45 \times 10^{-2}$
0.8	$1.70 \times 10^{-3}$ $8.98 \times 10^{-3}$ $2.52 \times 10^{-2}$	$9.19 \times 10^{-3}$ $2.76 \times 10^{-2}$	$1.05 \times 10^{-3}$ $9.22 \times 10^{-3}$ $3.05 \times 10^{-2}$
0.9	$1.32 \times 10^{-3}$ $6.81 \times 10^{-3}$ $1.13 \times 10^{-2}$	$1.11 \times 10^{-3}$ $8.16 \times 10^{-3}$ $1.36 \times 10^{-2}$	$1.09 \times 10^{-3}$ $7.06 \times 10^{-3}$ $1.25 \times 10^{-2}$
	$p=0.5$		
0.2	*	*	*
0.4	*	*	$6.68 \times 10^{-4}$
0.5	*	$1.03 \times 10^{-3}$	$2.21 \times 10^{-3}$
0.55	*	$3.757 \times 10^{-3}$	$6.90 \times 10^{-3}$
0.6	$1.29 \times 10^{-3}$	$5.28 \times 10^{-3}$	$1.08 \times 10^{-2}$
0.8	$8.31 \times 10^{-3}$ $1.74 \times 10^{-3}$	$8.40 \times 10^{-3}$ $1.81 \times 10^{-2}$	$8.54 \times 10^{-3}$ $1.91 \times 10^{-2}$
0.9	$1.32 \times 10^{-3}$ $6.60 \times 10^{-3}$ $1.44 \times 10^{-2}$	$1.21 \times 10^{-3}$ $6.72 \times 10^{-3}$ $1.20 \times 10^{-2}$	$1.44 \times 10^{-2}$ $1.28 \times 10^{-2}$ $1.20 \times 10^{-2}$

quantitatively pin down the minimum finger width and the  $p$  dependence of the forbidden region. An alternate approach suggested by Vanden-Broeck<sup>24</sup> for Taylor bubbles, which involves looking for bifurcation points at zero surface tension, might be useful for approaching this question.

With anisotropy, finger widths both below and above  $\frac{1}{2}$  are found. Again for small  $\gamma$  there are convergence difficulties. As  $\lambda$  increases, multiple solutions appear, and as in the Saffman-Taylor case we expect that at best one solution will be stable, leading to a unique finger shape. When  $\lambda$  approaches 1, our numerical method again has difficulties, but now due to inadequate resolution in the tail region. In fact, at  $\lambda=1$ , one must take account of the cusp at  $y \rightarrow -\infty$ , and a recent study by Karma<sup>25</sup> has treated a variant of this case successfully.

## VI. DISCUSSION

In the Hele-Shaw system, as  $\gamma$  is lowered the finger undergoes a transition to a more complicated pattern. The first mode to be excited is an antisymmetric one; eventually a symmetric, tip-splitting mode is also observed. It is fairly well established theoretically that (at least for capillary numbers that are not too large) these modes are linearly stable and are excited only when noise has exceeded a finite threshold. Experimental results on flow in

Hele-Shaw cells are consistent with this picture.

There is a simple argument that leads one to expect that any system with a solvability mechanism relying on exponentially small nonperturbative contributions might have finite noise instabilities. The key is that the difference between the allowed solutions and nearby disallowed solutions is proportional to  $e^{-c/\sqrt{\gamma}}$ . Therefore, if the selected  $\gamma^*$  turns out to be small, the solvability "signal" is also small. If the noise is larger than this signal, we might expect a more complicated time development of the interface. The most immediate consequence of this reasoning is that the noise threshold should obey the law

$$N^* \sim e^{-c/\sqrt{\gamma}},$$

with the same constant  $c$  which appears in the solvability mechanism. Just this dependence has been found by Ben-simon,<sup>19</sup> with approximately the same factor as that given in the solvability study of Ref. 26.

In the Hele-Shaw fluid flow system,  $\gamma$  is chosen at the experimenter's discretion and  $\lambda$  is measured. In channel growth, on the other hand,  $\lambda$  is fixed by the supersaturation boundary condition and  $\gamma$  is measured. In most crystals used for dendritic growth studies (e.g., succinonitrile) the anisotropy is fairly small,  $\epsilon \lesssim 10\%$ . This guarantees that whenever the supersaturation  $\lambda$  is picked in what would be the forbidden range at  $\epsilon=0$ ,  $\gamma^*$  will in fact be small. Hence, we might expect that as  $\lambda$  decreases at fixed anisotropy (or as the channel width is increased at fixed  $\lambda$ ), we will eventually leave the regime of a pure steady-state pattern.

Once we no longer have a needle crystal, what are the other possibilities? The experiments of Ref. 9 suggest that for some range of  $\lambda$  and  $\epsilon$  we would find sidebranching, perhaps induced by noise. That is, we expect that the character of the mode which is excited by the noise might change as we vary the system parameters. The Saffman-Taylor instability is controlled by tip-splitting modes which asymptotically decay exponentially to the original finger. A sidebranching system is dominated instead by modes which are peaked away from the tip, and therefore in a channel geometry obey the asymptotic dispersion law for a zero velocity planar interface. The latter statement implies that any such a mode will automatically have  $\omega \sim -ik$ , which implies stationarity in the laboratory frame of reference.

We do not as yet understand when the above scenario should occur. For example, are there ever real sidebranches at  $p=0$  as a function of  $\epsilon$ ? We do feel that this geometry is particularly convenient for trying to address this issue. Since the interface eventually approaches a plane, all eigenvectors of possible interest must approach plane waves; this is not true of the free dendrite problem which has power-law behavior asymptotically. We hope to report soon on the results of a stability calculation of the steady-state solutions discussed here.

## APPENDIX

In this appendix we apply the WKB method introduced originally by Langer<sup>27</sup> (and subsequently extended by

Shraiman,<sup>12</sup> Hong and Langer,<sup>13</sup> and Combescot *et al.*<sup>14</sup>) to study the dependence of  $\lambda$  on  $\gamma$  at finite anisotropy in the Saffman-Taylor limit  $p \rightarrow 0$ . These authors have shown that in the absence of anisotropy  $(\lambda - \frac{1}{2}) \rightarrow \gamma^{2/3}$  as  $\gamma \rightarrow 0$ . We have argued above that at finite  $\epsilon$ , there exist propagating steady-state fingers for all widths  $0 \leq \lambda \leq 1$ , and we now show how this behavior comes about within the WKB approximation. In the course of our calculations, we indicate which features of the  $\gamma=0$  solutions are necessary to obtain the asymptotic scaling of the finger width, an important consideration if this methodology is to be extended to systems such as channel growth with  $p \neq 0$ , directional solidification, and Taylor bubbles, where the continuum solutions with  $\gamma=0$  cannot be found analytically.

Following Shraiman,<sup>12</sup> consider the steady-state equation in the schematic form

$$F[y(x), \alpha] = 0, \quad (\text{A1})$$

where  $\alpha$  is an abbreviation for the parameters entering into the equation and boundary conditions (in the present case  $\epsilon$ ,  $\gamma$ , and  $\lambda$ ). Since the problem is translation invariant, if  $y(x)$  is a solution so is  $y(x) + y_0$  for any constant  $y_0$ . If we then expand  $F[y(x) + y_0, \alpha]$  for infinitesimal  $y_0$ , we find  $Ly_0 = 0$ , where the operator  $L \equiv \delta F / \delta y$ . Now consider varying the parameters  $\alpha$  infinitesimally along some trajectory; we expect a translation-invariant finger solution will continue to exist, which requires the perturbed operator  $L + \delta L$  to continue to have a constant zero mode. In lowest-order perturbation theory this requires

$$\hat{y}_0^\dagger \delta L y_0 = 0, \quad (\text{A2})$$

where the adjoint mode  $\hat{y}_0^\dagger$  obeys  $L^\dagger \hat{y}_0 = 0$ .

Note that the condition (A2) for the existence of finger solutions is similar but not identical to those stated previously. For example, Shraiman<sup>12</sup> requires the matrix element of  $L$  between the adjoint mode and  $\partial F / \partial \alpha$  to vanish, while Hong and Langer<sup>13</sup> require that the cusp magnitude in a certain WKB approximate solution vanish. As we shall see, the matrix element (A2) in the small- $\gamma$  limit takes the form of a WKB solution for  $\hat{y}_0^\dagger$  times a slowly varying and nonvanishing quantity, and the integrability condition is effectively the same in all approaches. The specific form of the slowly varying part is different, however, but this merely reflects the fact that we should make a systematic asymptotic expansion and match to a nonlinear "inner" problem. This point has already been discussed for local models<sup>28</sup> and for the Saffman-Taylor problem,<sup>14</sup> and will not be addressed further here.

Consider the steady-state equation in the form

$$\int ds' (\hat{n} \cdot \nabla G \gamma) d(\theta) \kappa = \frac{1}{\lambda} \int dx' G, \quad (\text{A3})$$

where  $d(\theta) = 1 - \epsilon \cos m \theta$  and we have shifted  $G$  as discussed at the end of Sec. II, and rescaled as indicated in (12). To obtain the adjoint equation, we suppose  $y(x)$  is the solution of (A3) and obtain the linearized equation by substituting  $y(x) + \delta(x)$  and expanding to first order in  $\delta$ :

$$\int ds'(\hat{\mathbf{n}} \cdot \nabla G)d(\theta) \frac{-\gamma \delta''(x')}{[1+y'(x)^2]^{3/2}} \\ = \frac{1}{\lambda} \int dx' \frac{\partial G}{\partial y'} [\delta(x') - \delta(x)].$$

We have dropped terms involving fewer derivatives of  $\delta$ , as these will be irrelevant in the small- $\gamma$  limit. The adjoint equation is, to the same level of approximation,

$$\int ds'(\hat{\mathbf{n}} \cdot \nabla G)d(\theta) \frac{\gamma \delta''(x')}{[1+y'(x)^2]^{3/2}} \\ = \frac{1}{\lambda} \text{P} \int dx' \frac{\partial G}{\partial y'} [\delta(x') + \delta(x)], \quad (\text{A4})$$

where P denotes a principal part integral. In analogy with the behavior of previously studied models, we look for rapidly oscillating solutions of the adjoint equation of the form

$$\delta(x) \sim \exp \left[ \frac{i}{\sqrt{\gamma}} \psi(x) \right] \quad (\text{A5})$$

in the limit  $\gamma \rightarrow 0$ . Substituting this ansatz into (A4), we evaluate the resulting integrals by residues. The leading contribution on the left-hand side comes from the singularity in  $G$  at  $x = x'$ , and we assume (subject to later verification) that the integration contour can be closed in the lower half plane. The contribution of other singularities in the complex plane is suppressed by the rapid oscillations produced by  $\delta$ . The left-hand side is then

$$\frac{\frac{1}{2} \gamma d(\theta) \delta''(x)}{[1+y'(x)^2]^{3/2}}.$$

(Note that the collapse to this form indicates that there is no structural difference between the one-sided model considered here and the symmetric model.) The term on the right-hand side proportional to  $\delta(x')$  can be evaluated similarly to give

$$\frac{-\frac{1}{2} i y'(x) \delta(x)}{1+y'(x)^2}.$$

The final term is more complicated because  $\delta$  comes outside the integral and we must also include the contributions of singularities at points  $x^*$ , where  $y(x^*) - y(x) = \pm i(x - x^*)$ . Assuming there is just one such point in each half plane, the last term in (A4) is

$$\left[ \frac{-\frac{1}{2} i y'(x)}{1+y'(x)^2} - \frac{\frac{1}{2}}{1+i y'(x^*)} \right] \delta(x).$$

In our subsequent arguments, we shall be concerned with  $x$  near  $x^*$ , in which case we obtain the WKB equation

$$\frac{\gamma d(\theta) \delta''(x)}{[1+y'(x)^2]^{3/2}} = - \frac{[1+i y'(x)] \delta(x)}{1+y'(x)^2}.$$

Substituting (A5) and keeping the leading term as  $\gamma \rightarrow 0$ , we obtain

$$\psi(x) = -i \int_0^x dx' (1+i y')^{3/4} (1-i y')^{1/4} [d(\theta)]^{-1/2},$$

where the normalization has been chosen so that  $\delta(0) = 1$ . Finally, we change variables to  $y'$ , and our final result for the solvability condition takes the form

$$I \equiv \int dx f(x) e^{i \psi(x)/\sqrt{\gamma}} = 0, \quad (\text{A6})$$

where  $f(x)$  is a slowly varying function and

$$\psi(x) = -i \int_0^{y'(x)} dz \frac{(1+iz)^{3/4} (1-iz)^{1/4}}{g(z)}, \quad (\text{A7})$$

where  $g(y') = y'' \sqrt{d(\theta)}$  and  $\theta(z) = \tan^{-1} z$ .

The scaling behavior of the solution follows from the singularities in the last expression for  $\psi$ . Note the saddle point in (A7) at  $y'(x) = i$ ; if  $g(z)$  has no singularities in the way, the integration contour can be simply deformed to pass through this saddle point, leading to an asymptotic estimate for  $I$  of the form

$$I \sim A \gamma^{-\alpha} e^{-B/\sqrt{\gamma}}$$

for some constants  $A$ ,  $\alpha$ , and  $B$ , and  $I$  never vanishes. On the other hand, if  $g$  has a zero on the line  $0 < z \leq i$ , the deformed contour will pass around this singularity and  $I$  will oscillate. Supposing the zero occurs at  $z = i(1-\sigma)$ , with  $0 < \sigma \ll 1$  and that the behavior of  $g$  in the neighborhood of  $z = i$  is  $g \rightarrow \chi(1+iz)^\phi$ , then the contribution of the extra contour is

$$\Delta \psi \sim -i \int_{i(1-\sigma)}^i dz \frac{1}{\chi} (1+iz)^{3/4-\phi} \sim \frac{1}{\chi} \sigma^{7/4-\phi}.$$

Let us first verify this result for pure dendritic growth. We take  $y = -x^2/2$  and  $m = 4$ , so that  $y''$  is constant and  $g \propto \sqrt{1-\epsilon \cos 4\theta(z)}$ . Using  $\cos 4\theta = 1 - 8z^2/(1+z^2)^2$ , we see that  $\sigma \sim \sqrt{\epsilon}$ ,  $\phi = -1$ , and  $\chi \sim \sqrt{\epsilon}$ , so  $\Delta \psi \sim \epsilon^{7/8}$ . The solvability condition that  $I$  vanish requires  $\Delta \psi/\sqrt{\gamma} = O(1)$ , and this requires  $\gamma \sim \epsilon^{7/4}$ . For the isotropic Saffman-Taylor problem,  $y(x) = 2(1-\lambda)/\pi \ln \pi x / 2\lambda$ , from which we obtain

$$g(z) = \frac{\pi(1-\lambda)}{2\lambda^2} \left[ 1 + \left( \frac{\lambda z}{1-\lambda} \right)^2 \right].$$

For  $\lambda \geq \frac{1}{2}$  there is a zero of  $g(z)$  at  $z = i(1-\lambda)/\lambda$  so that  $\sigma, \chi \sim \lambda - \frac{1}{2}$  and  $\phi = 0$ , and hence  $\gamma \sim (\lambda - \frac{1}{2})^{3/2}$ . Both of these special cases have been derived previously.<sup>12-14, 1, 29</sup>

For the finite anisotropy Saffman-Taylor problem, we use the same initial shape as above. For fixed  $\lambda \leq \frac{1}{2}$  the important singularity is that due to the  $\epsilon$ -dependent term, we again find  $\gamma \sim \epsilon^{7/4}$ . If instead we fix  $\epsilon$  and consider  $\lambda$  small, we have  $g(z) \sim \lambda^{-2}$  and the solvability condition requires  $\lambda \sim \gamma^{1/4}$ . These are the results quoted in the text.

It is remarkable that the only input to these scaling laws is the function  $g(z)$ , which depends on the analytic properties of  $y''$ , i.e., the initial shape extended to the complex plane. While this methodology is applicable to any of the fingered pattern problems of interest, we have been unable to devise a simple technique for the analytic continuation when the  $\gamma = 0$  problem is not analytically solvable.

- <sup>1</sup>D. Kessler, J. Koplik, and H. Levine, in *Patterns, Defects and Microstructure in Non-Equilibrium Systems*, Proceedings of the NATO A.R.W. Austin, Texas (March, 1986) (in press).
- <sup>2</sup>D. Kessler, J. Koplik, and H. Levine, *Physicochem. Hydro.* **6**, 507 (1985).
- <sup>3</sup>E. Ben-Jacob, N. Goldenfeld, G. Kotliar, and J. S. Langer, *Phys. Rev. Lett.* **53**, 2110 (1984).
- <sup>4</sup>J. M. Vanden-Broeck, *Phys. Fluids* **26**, 2033 (1983).
- <sup>5</sup>D. Bensimon, L. P. Kadanoff, S. Liang, B. Shraiman, and C. Tang, *Rev. Mod. Phys.* (to be published).
- <sup>6</sup>D. Meiron, *Phys. Rev. A* **33**, 2704 (1986).
- <sup>7</sup>D. Kessler, J. Koplik, and H. Levine, *Phys. Rev. A* **33**, 3352 (1986).
- <sup>8</sup>A. Karma, *Phys. Rev. Lett.* **57**, 858 (1986).
- <sup>9</sup>H. Honjo, S. Ohta, and Y. Sawada, *Phys. Rev. Lett.* **55**, 841 (1985).
- <sup>10</sup>E. Ben-Jacob, R. Godbey, N. D. Goldenfeld, J. Koplik, H. Levine, T. Mueller, and L. M. Sander, *Phys. Rev. Lett.* **55**, 1315 (1985).
- <sup>11</sup>P. G. Saffman and G. I. Taylor, *Proc. R. Soc. London, Ser. A* **245**, 312 (1958).
- <sup>12</sup>B. Shraiman, *Phys. Rev. Lett.* **56**, 2028 (1986).
- <sup>13</sup>D. C. Hong and J. S. Langer, *Phys. Rev. Lett.* **56**, 2032 (1986).
- <sup>14</sup>R. Combescot, T. Dombre, V. Hakim, Y. Pomeau, and A. Pumir, *Phys. Rev. Lett.* **56**, 2036 (1986).
- <sup>15</sup>P. Tabeling, G. Zocchi, and A. Libchaber (unpublished).
- <sup>16</sup>Preliminary experimental results indicate that in the presence of anisotropy in channel solidification, finger widths below  $\frac{1}{2}$  are found; E. Ben-Jacob (private communication).
- <sup>17</sup>C. W. Park and G. M. Homsy, *Phys. Fluids* **28**, 1583 (1985).
- <sup>18</sup>A. J. DeGregoria and L. W. Schwartz (unpublished).
- <sup>19</sup>D. Bensimon, *Phys. Rev. A* **33**, 1302 (1986).
- <sup>20</sup>R. Pieters and J. S. Langer, *Phys. Rev. Lett.* **56**, 1948 (1986).
- <sup>21</sup>D. P. Woodruff, *The Solid-Liquid Interface* (Cambridge University Press, Cambridge, England, 1973).
- <sup>22</sup>IMSL Inc., Houston, TX (1984).
- <sup>23</sup>J. W. McLean and P. G. Saffman, *J. Fluid Mech.* **102**, 455 (1982).
- <sup>24</sup>J. M. Vanden-Broeck, *Phys. Fluids* **29**, 2298 (1986).
- <sup>25</sup>A. Karma, *Phys. Rev. A* **34**, 4353 (1986).
- <sup>26</sup>D. Kessler and H. Levine, *Phys. Rev. A* **32**, 1930 (1980); **33**, 2621 (1986); **33**, 2634 (1986).
- <sup>27</sup>J. S. Langer, *Phys. Rev. A* **33**, 435 (1986); see also B. Caroli, C. Caroli, B. Roulet, and J. S. Langer, *ibid.* **33**, 442 (1986).
- <sup>28</sup>R. Dashen, D. Kessler, H. Levine, and R. Savit, *Physica D* **21**, 371 (1986).
- <sup>29</sup>D. C. Hong and J. S. Langer (unpublished).